APPLIED ORGANOMETALLIC CHEMISTRY
Appl. Organometal. Chem. 2002; **16**: 506–516 **Materials, Nanomaterials and Synthesis** **AOC**

N-Pyrrolyl-[*N,N,N*]-bis(imino)pyridyl iron(II) and cobalt(II) olefin polymerization catalysts[†]

Christoph Amort[1], Michael Malaun[1], Alexander Krajete[1], Holger Kopacka[1], Klaus Wurst[1], Maria Christ[2], Dieter Lilge[3], Marc O. Kristen[2,3] and Benno Bildstein[1]*

[1]Institute of General, Inorganic and Theoretical Chemistry, University of Innsbruck, Innrain 52a, A-6020 Innsbruck, Austria
[2]BASF AG, Polymer Laboratory, D-67056 Ludwigshafen, Germany
[3]Basell Polyolefine GmbH, D-67056 Ludwigshafen, Germany

Received 22 November 2001; Accepted 27 May 2002

A series of new [*N,N,N*] 2,6-bis(imino)pyridyl iron and cobalt halide complexes as precatalysts for the homo- and co-polymerization of ethylene has been synthesized and evaluated for their catalytic performance. The novel key structural feature of these [*N,N,N*]MCl_2 catalysts is their peripheral substitution with bulky *N*-heterocyclic groups, including substituted *N*-pyrrolyl, *N*-indolyl, *N*-carbazolyl, and *N*-triazolyl moieties. The synthesis starts with the corresponding *N*-amino-*N*-heterocycles, which were prepared by a modified Paal–Knorr condensation of 1,4-diketones with mono-protected hydrazines, or by electrophilic amination of benzannelated azoles. Condensation with 2,6-diacetylpyridine or 2,5-diformylthiophene afforded 14 different terdentate ligands, and complex formation with iron(II), iron(III), cobalt(II) yielded 23 different precatalysts. A single crystal structure analysis of one representative showed that these paramagnetic complexes have a distorted trigonal bipyramidal structure with orthogonal sterically shielding *N*-azolyl groups. All the methylalumoxane-activated iron(II) and cobalt(II) complexes with *N*-pyrrolyl, *N*-indolyl, and *N*-carbazolyl substituents are highly active catalysts for the homo- and co-polymerization of ethylene, producing polymers with comparatively narrow molecular weight distributions and with a wide range of molecular weights, dependent on the substitution pattern of the peripheral *N*-azolyl substituents. The observed microstructures of the polymers vary from very highly branched to mostly linear, giving access to oligomers and polymers with an unusual broad spectrum of macroscopic physical properties. Copyright © 2002 John Wiley & Sons, Ltd.

KEYWORDS: iron; cobalt; N ligands; *N*-amino pyrrole; olefin; polymerization

INTRODUCTION

Important progress has been achieved in the last few years in the development of new non-metallocene late transition metal catalysts for the cationic polymerization of α-olefins (for reviews, see Refs 1–4). Among the most significant findings in this area are the recent reports by the groups of Gibson[5–7] and Brookhart[8,9] on novel highly active and versatile catalysts based on tridentate 2,6-bis(imino)pyridyl iron and cobalt halide complexes. Remarkable high activities for the polymerization of ethylene, similar to those of the most active Ziegler–Natta systems, have been reported, and the physical properties of the polyolefins produced can be tailored by the choice of the metal center and the substitution pattern of the ligand backbone. Not surprisingly, this family of catalysts and their industrial application is of considerable commercial interest, as evidenced by a number of recent patents concerning homo- and co-polymerizations of ethylene[10,11] and propylene.[12,13]

From the experimentally established activity–structure relationships,[5–13] and from a number of theoretical studies,[14–17] the key structural feature of the ligand framework of these catalysts is apparently sufficient steric shielding of the active cationic center in the axial positions, effected by the use of bulky ortho-substituted aryl groups (e.g. 2,6-diisopro-

---

*Correspondence to: B. Bildstein, Institute of General, Inorganic and Theoretical Chemistry, University of Innsbruck, Innrain 52a, A-6020 Innsbruck, Austria.
E-mail: benno.bildstein@uibk.ac.at

[†]This paper is based on work presented at the XIVth FECHEM Conference on Organometallic Chemistry held at Gdansk, Poland, 2–7 September 2001.

Contract/grant sponsor: BASF AG, Ludwigshafen.

pylphenyl) attached to the imine nitrogen atoms of the bisimine/pyridine chelating ligand. In contrast to these reported catalysts, which contain a number of variously substituted *N-aryl* substituents,[5–13] we have been using bulky *N-heteroaromatic* substituents (*N*-pyrrolyl, *N*-indolyl, *N*-carbazolyl, etc.) aiming at a further improvement in the catalytic performance of these types of non-metallocene catalyst.

During the preparation of this manuscript, we became aware of a similar approach disclosed recently by the Eastman Chemical Company[18] and by the Gibson group.[19,20] The *N*-heteroaromatics have been selected because of their isoelectronic properties (compare pyrrole and benzene) and their similar steric bulk (compare 2,5-disubstituted pyrrole and 2,6-disubstituted benzene). As will be seen in the following, this design principle gives access to a new family of improved catalysts that show superior activity and which produce homo- and co-polymers with a broad spectrum of tunable physical properties.[21]

RESULTS AND DISCUSSION

Synthesis and properties of the ligands and metal complexes

From a retrosynthetic point of view, the synthetic sequence for the preparation of *N*-azolyl 2,6-bis(imino)pyridyl metal complexes as precatalysts for the polymerization involves (i) synthesis of *N*-amino azoles, (ii) condensation of 2,6-diacetylpyridine with two equivalents of *N*-amino azole, and (iii) complexation of the appropriate transition metal halide with the terdentate ligands. The latter two reactions presented no real difficulties, and were more or less analogous to the published preparation of *N*-aryl 2,6-bis(imino)pyridyl complexes,[5–13] but the synthesis of *N*-amino azoles needed more work.

N-Amino-pyrroles

The most general method to synthesize 2,5-disubstituted *N*-amino pyrroles consists in a modified Paal–Knorr condensation[22] starting from 1,4-diketones and a mono-protected hydrazine (Scheme 1). Symmetric 1,4-diketones may be prepared from methylketones by a copper-mediated radical C–C coupling reaction[23] (metalation of the methylketone by lithium diisopropylamide, transmetalation with $CuCl_2$, and thermal decomposition to the corresponding radicals with concomitant dimerization), albeit with yields that are rather poor. Nevertheless, the starting materials are inexpensive and the products can be isolated by fractional distillation; therefore, this method is of some value. An alternative synthetic approach consists of the reaction of Grignard reagents with succinyl dichloride or alkyl succinate, respectively catalyzed by iron(III) acetylacetonate[24] or Li_2MnCl_4,[25] but in our hands these methods were much inferior to the dimerization of copper methylketones.

However, the most versatile and useful preparation of 1,4-diketones is the Stetter reaction:[26–29] Umpolung of aldehydes with cyanide or with *N*-heterocyclic carbenes followed by reaction with vinyl ketones allows the convenient one-pot preparation of symmetric and unsymmetric 1,4-diketones on a large scale (>20 g).

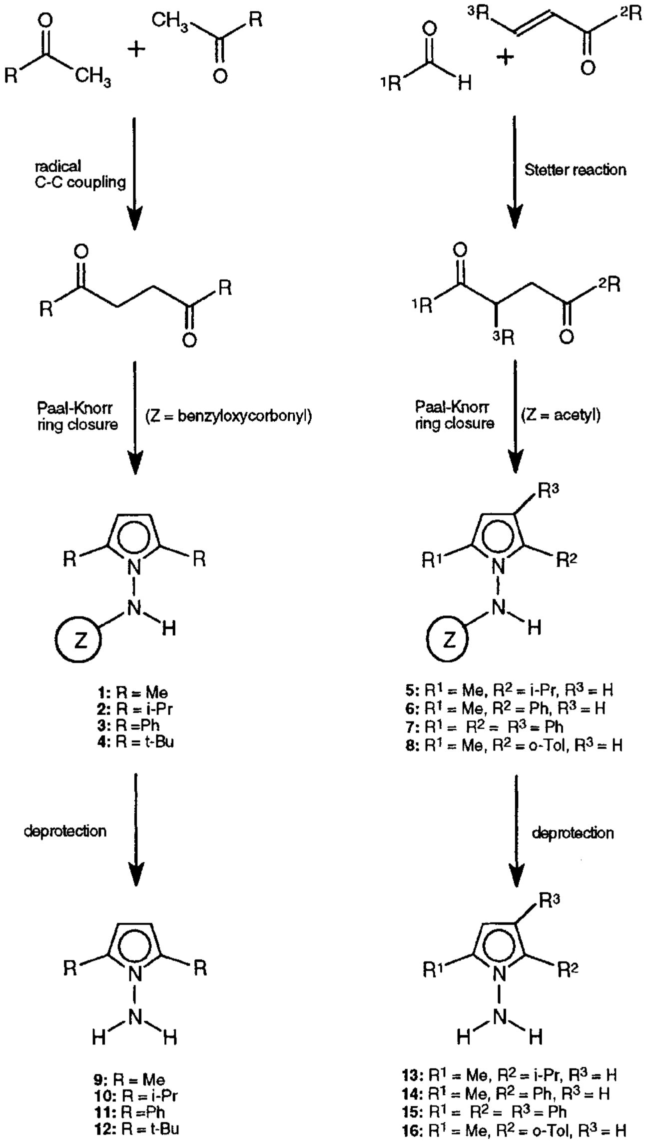

Scheme 1. Synthesis of *N*-aminopyrroles **9–16** (Me = methyl, i-Pr = isopropyl, Ph = phenyl, t-Bu = t-butyl, o-Tol = orthotolyl).

With these various 1,4-diketones in hand, the Paal–Knorr condensation with protected hydrazines gives access to the corresponding *N*-protected *N*-aminopyrroles **1–8** without difficulties. In contrast to the reported procedure, which uses the rather exotic protecting groups [$Cl_3CCH_2OC(O)$, $Me_3SiCH_2CH_2OC(O)$],[22] we used the more common protecting groups benzyloxycarbonyl or acetyl, respectively, with similar results. In terms of yield of products, the benzyloxycarbonyl group (**1–4**: 66–89% yield) is prefered over the acetyl group (**5, 6**: 37–53% yield), but in the

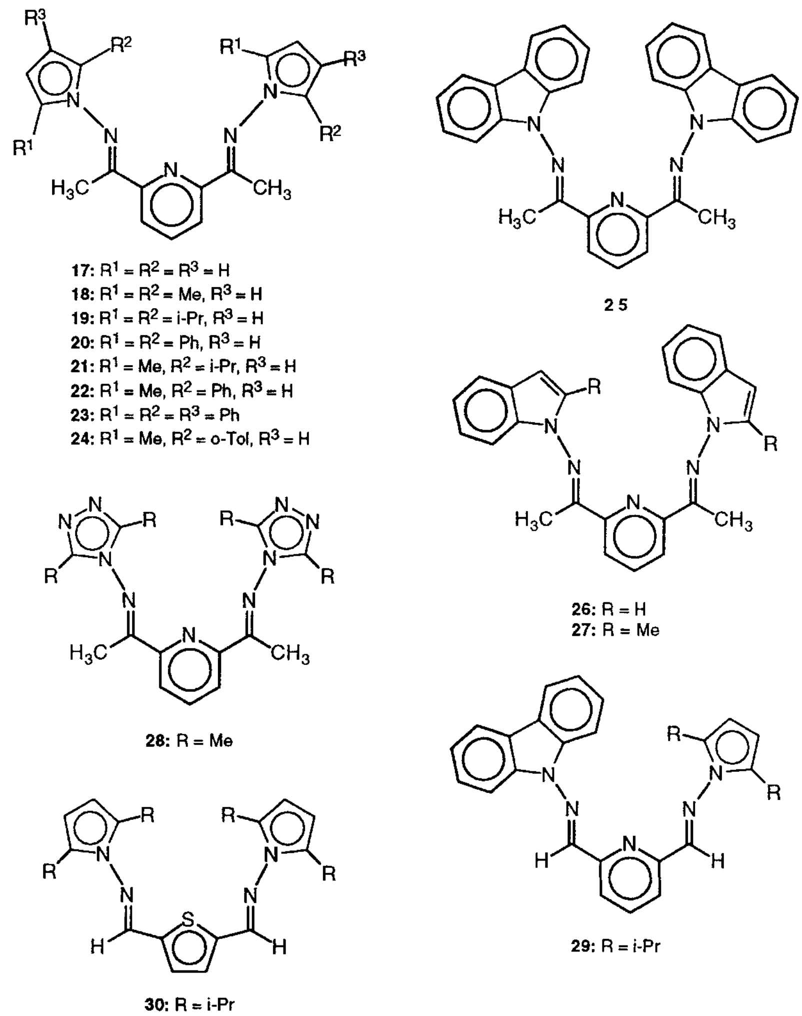

Figure 1. Overview of ligands **17**–**30** (Me = methyl, i-Pr = isopropyl, Ph = phenyl, o-Tol = orthotolyl).

subsequent deprotection step the acetyl moiety is easier to cleave. The *N*-aminopyrroles **9**–**16** were obtained from these amides in 80–95% yield by alkaline hydrolysis (1–36 h) with a KOH-saturated refluxing ethylene glycol solution. This convenient but rather drastic deprotection protocol shows also that *N*-aminopyrroles are quite stable compounds. The high stability of aminopyrroles **9**–**16** is without doubt due to the fact that both α-positions are blocked in these 2,5-disubstituted pyrroles. Interestingly, the parent member of this family of compounds, unsubstituted *N*-amino-pyrrole, is the only commercially available *N*-amino-azole, although it is the least stable compound in this series. In summary, *N*-amino-2,5-disubstituted pyrroles with a wide range of substituents can be conveniently prepared on a large scale. The only limitation of this method is the availability of the starting 1,4-diketones, which in turn are most easily accessible by the Stetter condensation.

N-Amino-indoles, -carbazoles, and -triazoles

To extend further the substitution pattern of these building blocks, analogous and/or benzannelated *N*-amino-*N*-heterocycles were prepared. (i) Electrophilic amination of indole, 2-methylindole, and carbazole using hydroxylamine-*O*-sulfonic acid yielded the corresponding *N*-amino-indole, -2-methylindole, and -carbazole respectively, according to published methods.[30–33] However, applying the same reaction conditions to 2,7-dimethylindole or dibenzazepine (iminostilbene) failed, most likely due to steric hindrance in these cases. (ii) 2,5-Disubstituted 1-amino-3,4-triazoles are isostructural to 2,5-disubstituted *N*-aminopyrroles. Such symmetric triazoles are very easily obtained from the condensation of hydrazine with carboxylic acids without the need to use a monoprotected hydrazine. One example, 2,5-dimethyl-1-amino-3,4-triazole, was synthesized by condensing acetic acid with hydrazine according to literature procedures.[34,35]

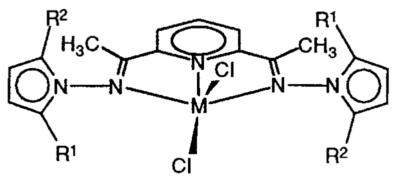

31a: $R^1 = R^2 = H$, M = Fe(II)
31b: $R^1 = R^2 = H$, M = Co(II)
32a: $R^1 = R^2 = Me$, M = Fe(II)
32b: $R^1 = R^2 = Me$, M = Co(II)
33a: $R^1 = R^2 =$ i-Pr, M = Fe(II)
33b: $R^1 = R^2 =$ i-Pr, M = Co(II)
34a: $R^1 = Me$, $R^2 =$ i-Pr, M = Fe(II)
34b: $R^1 = Me$, $R^2 =$ i-Pr, M = Co(II)
35a: $R^1 = Me$, $R^2 = Ph$, M = Fe(II)
35b: $R^1 = Me$, $R^2 = Ph$, M = Co(II)
36a: $R^1 = Me$, $R^2 =$ o-Tol, M = Fe(II)
36b: $R^1 = Me$, $R^2 =$ o-Tol, M = Co(II))

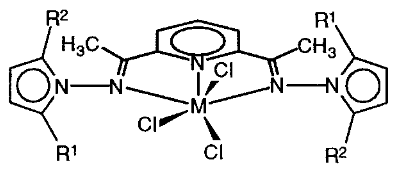

32c: $R^1 = R^2 = Me$, M = Fe(III)
33c: $R^1 = R^2 =$ i-Pr, M = Fe(III)

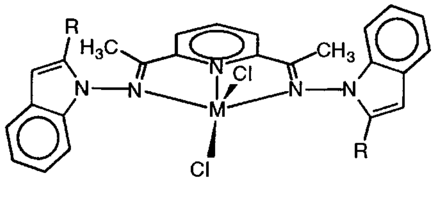

37a: R = H, M = Fe(II)
37b: R = H, M = Co(II)
38a: R = Me, M = Fe(II)
38b: R = Me, M = Co(II)

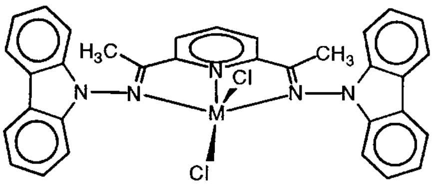

39a: M = Fe(II)
39b: M = Co(II)

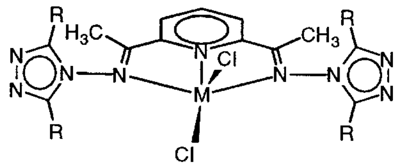

40a: R = Me, M = Fe(II)

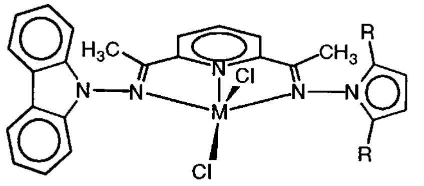

41a: R = Me, M = Fe(II)

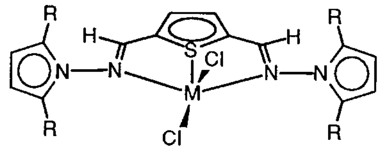

42b: R = Me, M = Co(II)

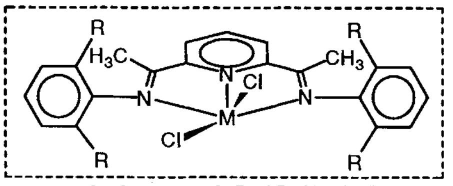

lead structure A: R = i-Pr, M = Fe(II)

Figure 2. Overview of metal complexes **31a–42b** [numbering: **a**, M = Fe(II); **b**, M = Co(II); **c**, M = Fe(III)].

By these synthetic methods, 12 different *N*-amino-*N*-heterocycles have been obtained in total. Together with the commercially available unsubstituted *N*-amino-pyrrole, 13 different *N*-amino-azoles are thus available as building blocks. Their properties—with regard to their intended use as steering groups in the ligand backbone of the olefin polymerization catalysts—differ in terms of: (i) steric bulk of the substituents (hydrogen, methyl, isopropyl, t-butyl, phenyl, orthotolyl); (ii) symmetry (symmetric *N*-amino-pyrrole, **9–12**, *N*-aminocarbazole, and 2,5-dimethyl-1-amino-3,4-triazole versus asymmetric **13–16**, *N*-amino-indole and *N*-amino-2-methylindole; (iii) electronic properties (pyrroles versus benzannelated *N*-heterocycles).

N-Azolyl-containing tridentate ligands

The bis(imino)pyridyl ligands were easily synthesized by reaction of 2,6-diacetylpyridine with two equivalents of heterocyclic amine; these condensations were performed under acidic conditions, either in methanolic solution with catalytic amounts of formic acid or in refluxing propionic acid in the case of less reactive components. In this manner, 13 different [*N*,*N*,*N*] bis(imino)pyridyl ligands (**17–29**) were prepared (Fig. 1). However, attempting the condensation between 2,5-di-t-butyl-*N*-aminopyrrole (**12**) and 2,6-diacetylpyridine met with failure, indicating that the two very bulky t-butyl substituents are not compatible with this [*N,N,N*] ligand framework. Whereas all the ligands **17–28** are symmetric in terms of bearing the same *N*-azolyl moiety on the two imine nitrogen atoms, one example of an asymmetric ligand with different *N*-substituents (**29**) was made by first condensing one equivalent of *N*-aminocarbazole to afford the corresponding monoimine, which was reacted in a second step with *N*-aminepyrrole (**10**). In general, in all these condensations the monoimine was formed very quickly, whereas the second imination proceeded much more slowly, thereby allowing, in principle, easy access to such asymmetric ligand backbones. Furthermore, an analogous condensation of 2,5-diformylthiophene with *N*-aminopyrrole (**10**) afforded the additional [*N,S,N*] ligand **30**, giving 14 different ligands comprising [*N,N,N*] and [*N,S,N*] ligand frameworks containing variously substituted peripheral *N*-heterocyclic substituents.

Metal complexes

The complexes **31a–42b** (Fig. 2) were synthesized in good yield from the ligands **17–30** by reaction with the appropriate metal halide ($FeCl_2$, $CoCl_2$, $FeCl_3$). In addition, for direct comparison of the performance of these precatalysts in olefin polymerizations under experimentally identical conditions [monomer pressure, molar ratio of methylalumoxane (MAO), reaction time, temperature, etc.], one of the most productive catalysts of the groups of Gibson[5–7] and Brookhart,[8,9] [2,6-diacetylpyridine-bis(2,6-diisopropylphenyl)imine]$FeCl_2$ (**A**), was synthesized according to reported methods.[5–13] In fact, this system served as the lead structure **A** in the beginning of this work (see Fig. 2).

The ligands **17–30** differ in their ligating properties. Almost all of the pyrrole-, indole-, and carbazole-containing systems afforded stable iron(II) and cobalt(II) complexes (most, but not all, possible metal/ligand combinations have been realized on a preparative scale), the only exceptions are ligands **20** and **23**, which contain only aryl substituents. This indicates that two pairs of ortho-phenyl groups on the *N*-pyrrolyl substituents impose too much steric hindrance and/or are too electron-withdrawing for the corresponding [*N,N,N*] metal complex. Interestingly, the *N*-triazolyl ligand **28** formed an iron(II) complex but no stable cobalt(II) complex; this is in contrast to thiophene ligand **30**, which yielded a cobalt(II) but no iron(II) complex. The two iron(III) precatalysts **32c** and **33c** were synthesized to evaluate the dependence of the polymerization performance on the oxidation state of the metal center. In total, 23 different *N*-azolyl complexes were prepared with the aim of a thorough structure–activity screening in direct comparison with *N*-aryl bis(imino)pyridyl complex **A**.

All the complexes **31a–42b** are: (i) deeply colored, mostly dark green for iron(II) and dark brown for cobalt(II); (ii) thermally very stable, no melting or decomposition is observed up to 300 °C; and (iii) paramagnetic, thereby preventing useful NMR analysis. These properties parallel those of Gibson's[5–7] and Brookhart's[8,9] *N*-aryl bis(imino)pyridyl complexes.

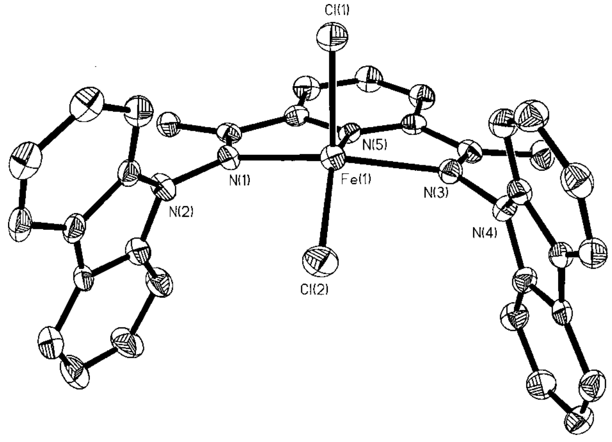

Figure 3. Molecular structure of iron complex **39a**, hydrogen atoms and solvent molecules are omitted for clarity. Selected bond lengths (pm): Fe(1)—N(1) = 220.2(4), Fe(1)—N(3) = 222.2(4), Fe(1)—N(5) = 207.9(5), Fe(1)—Cl(1) = 230.9(2), Fe(1)—Cl(2) = 225.9(2), N(1)—N(2) = 140.3(6), N(3)—N(4) = 141.8(6). Selected angles (deg): N(1)—Fe(1)—N(5) = 73.5(2), N(3)—Fe(1)—N(5) = 73.0(2), N(1)—Fe(1)—N(3) = 143.1(2), N(5)—Fe(1)—Cl(1) = 96.69(12), N(3)—Fe(1)—Cl(1) = 100.12(12), N(1)—Fe(1)—Cl(1) = 98.56(12), N(5)—Fe(1)—Cl(2) = 138.67(12), N(3)—Fe(1)—Cl(2) = 95.66(13), N(1)—Fe(1)—Cl(2) = 99.47(13).

For one representative of this family of precatalysts (**39a**), suitable single crystals for an X-ray structure analysis were obtained. Figure 3 shows the molecular structures of iron(II) complex **39a**; selected bond lengths and angles are given in the figure caption. The metal is coordinated in a distorted trigonal bipyramidal geometry to the three nitrogen atoms N(1), N(3), and N(5) of the bis(imino)pyridyl ligand and to two chlorine atoms; furthermore, the metal is clearly displaced from the [*N,N,N*] ligand plane by 40.6(4) pm. The bond distance of the pyridyl nitrogen is significantly shorter [N(5)−Fe(1) = 207.9(5) pm] than the distances of both imino nitrogen atoms [N(1)−Fe(1) = 220.2(4), N(3)−Fe(1) = 222.2(4) pm], and the two chlorine substituents have more or less similar metal–chlorine bond lengths [Cl(1)−Fe(1) = 230.9(2), Cl(2)−Fe(1) = 225.9(2) pm]. The planes of the sterically shielding *N*-carbazolyl groups are roughly orthogonal to the plane of the [*N,N,N*] bis(imino)pyridyl ligand backbone [78.5(3) and 75.1(2) °] and the *N*-carbazolyl moieties are planar in accordance with the sp^2 hybridization of the nitrogen atoms N(2) and N(4) in these *N*-heterocycles. All these structural features of **39a** are quite similar to those of Gibson's *N*-aryl bis(imino)pyridyl complexes,[5–7] indicat-

Table 1. Results of polymerizations[a]

Precatalyst	Amount of Fe/Co (μmol)	Comonomer	Amount of polymer[b] (g)	Activity [g polymer/(mmol Fe/Co) × h]	η[d] (dl/g^{-1})	T_M[e] (°C)	M_w[f]	M_n[f]	M_w/M_n[f]	Density (g/cm^{-3})
				Iron catalysts						
A[c]	100	–	32	320	2.72	135	318 385	7036	45	0.9596
A[c]	100	Hexene	14.5	145	2.71	138	245 448	4172	59	0.9625
31a	50	–	Trace							
32a	100	–	56.5	565	0.1	118	3401	1273	2.7	0.9241
32a	100	Hexene	69	690	0.1	117	3251	1440	2.3	0.9283
32c	50	–	1.0	20	0.1	117	2281	847	2.7	
33a	100	–	19	190	1.6	131	112 907	6483	17.4	0.9600
33a	50	Hexene	20.2	404	2.45	131	205 544	9298	22.1	0.9541
33c	50	–	Trace							
34a	50	–	4	80	0.44	120	14 084	1158	12.2	0.9177
34a	50	Hexene	49	980	0.61	121	29 937	1849	16.2	0.924[g]
35a	50	–	3.6	72	0.22	121	5438	1320	4.1	0.9338
35a	50	Hexene	3.7	74	0.21	119	5956	1224	4.9	0.9317
36a	50	–	1.5	30	0.31	123	8183	1329	6.2	0.9387
36a	50	Hexene	4.8	96	0.18	119	4737	1356	3.5	0.9387
37a	50	–	3.3 (oil)	66						
38a	50	–	16	320	0.06	63	1509	727	2.1	0.8913
38a	50	Hexene	15.5	310	0.12	63	1477	839	1.8	0.9061
39a	50	–	16 (oil)	320						
39a	50	Hexene	46 (oil)	920						
40a	50	–	Trace							
41a	50	–	0.5	10	0.11	76	1762	903	2.0	
41a	50	Hexene	12.5	250	0.05	60	1039	497	2.1	
				Cobalt catalysts						
31b	50	–	Trace							
32b	100	–	1	10	0.1	118	3582	1000	3.6	0.9271
32b	100	Hexene	24	240	0.05	83	879	659	1.3	0.9247
33b	100	–	5	50	0.45	127	13 600	3181	4.3	0.9605
33b	50	Hexene	0.6	6	0.84	126	9564	2735	3.5	0.9721
34b	50	–	8.6	172	0.27	124	4985	1949	2.6	0.9563
34b	50	Hexene	11.5	230	0.17	123	4565	1796	2.5	0.9528
35b	50	–	11.2 (oil)	224						
35b	50	Hexene	24.2 (oil)	482						
36b	50	–	0.6 (oil)	12						
36b	50	Hexene	1.5 (oil)	30						
38b	50	–	0.2	4	0.13	120	5896	1478	4.0	0.9333
38b	50	Hexene	0.6	12	0.1	65	1323	719	1.8	0.8948
39b	50	–	2 (oil)	40						
39b	50	Hexene	2.5 (oil)	50						
42b	50	–	0.2 (oil)	4						
42b	50	Hexene	0.1 (oil)	2						

[a] Conditions: 100 equivalents MAO, ethylene 40 l h^{-1}, 30 °C, 1 h.
[b] Yields of oils refer to isolated yields.
[c] Lead structure/complex **A**.
[d] Viscosity, determined in decalin at 180 °C.
[e] Determined by differential scanning calorimetry.
[f] Determined by gel permeation chromatography.
[g] Incorporation of 2.4 mol% hexene, determined by IR.

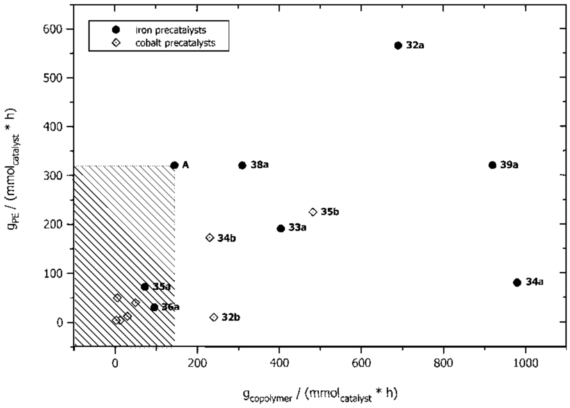

Figure 4. Comparison of the activities of iron and cobalt precatalysts in the homo- and co-polymerization of ethylene and ethylene/1-hexene respectively.

ing only subtle differences between *N*-azolyl and *N*-aryl bis(imino)pyridyl metal halide precatalysts from a structural point of view.

Polymerization studies

Polymerization of ethylene

The general catalytic performance of the metal complexes **31a**–**42b** in cationic polymerizations of olefins was compared by a standard polymerization procedure. The complexes **31a**–**42b** (50 or 100 μmol) were activated with 100 mole equivalents of MAO in toluene solution, the ethylene feed was adjusted to 40 l h^{-1}, the polymerizations were allowed to proceed for 1 h at a temperature of 30 °C, the mixture was quenched with methanol, and the solid polymer was washed and dried *in vacuo*. When no solid polymer was formed, the organic layer was evaporated on a rotary evaporator, yielding an oily residue. Table 1 summarizes the polymerization results and gives some relevant properties of the polymers. Figure 4 shows the productivity of both families of precatalysts in the homopolymerization of ethylene and in the copolymerization of ethylene with 1-hexene. From these data, the following general trends can be deduced.

(i) All the precatalysts **31a**–**39b** and **41a** containing *N*-pyrrolyl, -indolyl, -carbazolyl substituents showed remarkable high activities, similar to those of Gibson's or Brookhart's *N*-aryl-substituted catalysts. The triazolyl complex **40a** and the thiophene complex **42b** showed only low activity.

(ii) Iron(II) catalysts **31a**–**41a** are, in general, more active by a factor of 10–100 in comparison with cobalt(II) complexes **31b**–**39b**. The low activity of iron(III) complexes **32c** and **33c** suggests that only iron(II) but not iron(III) species are active in catalysis; the low activity of **32c** is most likely due to reduction of iron(III) by alkyl aluminum compounds.

(iii) Increasing steric bulk of the peripheral *N*-azolyl groups leads to polymers with higher molecular weight, whereas a decrease of the steric shielding results in higher activity. The highest activity for the homopolymerization of ethylene is shown by the 2,5-dimethylpyrrolyl complex **32a**, with an almost doubled productivity in direct comparison to the lead complex **A**. It is also interesting to note that in the case of Gibson's and Brookhart's catalysts the analogous 2,4,6-trimethylphenyl iron(II) complex is the most active complex under the conditions examined.[5–13] However, in the cobalt series, the most productive complex is **35b** with 2-methyl-5-phenyl-pyrrolyl substituents.

(iv) The molecular weights of the polymers obtained are, in general, somewhat lower than those of the polymers derived from Gibson's and Brookhart's *N*-aryl catalysts,[5–9] but the polydispersities are much narrower. The cobalt complexes yield mainly oils of low molecular weight; one extreme case is complex **39b**, which yields highly branched oligomers with a chain length of less than 18 carbon atoms, as indicated by gas chromatography analysis.

(v) Oligomers produced with the *N*-pyrrol-derived complexes differ quite substantially from the oligomers obtained from the *N*-aryl-based systems. Whereas the latter catalysts yield strictly linear oligomers,[7] here a significant degree of branching is observed. The polymer obtained is a complex mixture of different, low molecular weight oligomers. For example, a detailed NMR analysis of the polyethylene produced by precatalyst **39a** showed 1.1% vinyl, 0.2% vinylidene, 4.3% cis/trans double bonds with a branching (endgroups per 1000 carbon atoms) of 19 methyl, 71 ethyl, 11 butyl, 80 alkyl $\geq C_6$, and 181 total methyl groups. The amount of double bonds—especially the internal double bonds—is quite remarkable. Obviously, no single termination pathway is responsible for the formation of the polymers.

Copolymerization of ethylene with 1-hexene

Copolymerizations of MAO-activated complexes **30a**–**40b** were performed in a similar manner to that described above for toluene solution at 30 °C, but liquid 1-hexene was admixed to the solution. As can be seen from inspection of Table 1, these *N*-azolyl catalysts are extremely efficient in incorporating the comonomer 1-hexene (Fig. 4). The most productive catalysts are the iron(II) complexes with *N*-(2-methyl-5-isopropyl)-pyrrolyl, *N*-carbazolyl, *N*-(2,5-dimethyl)-pyrrolyl substituents and the cobalt(II) complex with 2-methyl-5-phenyl-pyrrolyl substituents (**34a**: 980; **39a**: 920; **32a**: 690; **35b**: 482 g polymer/mmol Fe/Co × h), yielding low molecular weight polymers with narrow to broad polydispersities, dependent on the substitution pattern. It is noteworthy that the iron(II) complex **34a** produces a copolymer with 2.4 mol% hexene incorporated. So far, complexes with the ligand type examined were known to incorporate only marginal amounts of hexene, if any.

Polymerization of propylene

Complex **32a**, which was one of the most productive in the homopolymerization of ethylene, served as the test case for the polymerization of propylene. Under similar experimental conditions as described above (with propylene instead of ethylene as the monomer), 15 g of an oily polymer was obtained, corresponding to an activity of 300 g polypropylene/mmol Fe × h). The ^{13}C NMR spectrum of the polymer clearly showed an atactic structure. In addition, a variety of endgroups, both saturated and unsaturated, could be observed, indicating that no single termination pathway takes place.

Mechanistic considerations

From the results discussed above, and from the properties of the polymeric products, one might speculate on the mechanism by which these catalysts oligomerize or polymerize ethylene and/or 1-hexene. Assuming that these MAO-activated catalytic species are intermediate cationic alkyl complexes, there has to be a delicate balance between simple insertion of the monomer (resulting in a linear polymer) and β-hydride elimination and re-addition (resulting in branching). The mostly highly branched microstructure of the polyethylene produced by catalyts **31a–42b**, dependent on the substitution pattern of the precatalysts, suggests that either the latter process, 'chain-walking', is quite important, or that re-incorporation of the grown oligomer chains occurs. This is in marked contrast to Brookhart's and Gibson's bis(imino)pyridyl iron and cobalt complexes, which produce highly linear polyethylene,[5–9] but quite analogous to 1,2-diimine nickel and palladium complexes, which yield mainly branched polymers.[1–4] There is no straightforward explanation for this behavior of catalysts **31a–42b**, but it is interesting and significant that the seemingly slight modification of the peripheral substituents (*N*-azolyl versus *N*-phenyl) has such a dramatic effect on the microstructure and physical properties of the polymers. Obviously, the electronic effects imposed by the peripheral *N*-heterocyclic substituents (compared with *N*-aryl) have to be responsible for these results, because there are only marginal steric differences between five- and six-membered rings as peripheral steering groups.[19,20]

SUMMARY

A new family of non-metallocene late transition metal catalysts of the bis(imino)pyridyl iron(II) and cobalt(II) type has been synthesized and screened for their catalytic performance in the homo- and co-polymerization of ethylene. Conceptually, peripheral *N*-imino-substitution with various *N*-amino heterocycles was used as the catalyst-design principle in these complexes.

Synthetically, the *N*-amino heterocycles were prepared either by a modified Paal–Knorr condensation of 1,4-diketones (obtained by a radical C–C coupling of methylketones, or by Stetter condensation of aldehydes with vinyl ketones), or by electrophilic *N*-amination of annelated azoles. The precatalyts were synthesized by condensation of the *N*-amino heterocycles with 2,6-diacetylpyridine followed by complex formation with iron and cobalt halides, yielding a set of 23 different precatalysts with varying substitution patterns in terms of steric bulk, symmetry, and electronic properties of the *N*-imino substituents. Polymerization studies showed that these complexes are highly productive catalysts for the homopolymerization of ethylene and unusually active catalysts for the copolymerization of ethylene with 1-hexene, yielding polymers and oligomers with tunable physical properties in terms of molecular weight, polydispersity, viscosity, and density. The polymers have a microstructure ranging from more or less linear to highly branched, depending on the substitution pattern of the precatalysts.

EXPERIMENTAL

Materials

1-Aminopyrrole was obtained from Tokyo Kasei Kogyo, Japan. Non-commercially available 1,4-diketones as starting materials for the Paal–Knorr synthesis of substituted *N*-amino pyrroles[22] were prepared according to published procedures.[23,26–29] *N*-Amino-indole, -(2-methyl)indole, and -carbazole were synthesized from indole, 2-methylindole, and carbazole respectively, using hydroxylamine-*O*-sulfonic acid as electrophilic amination reagent.[30–33] *N*-Amino-2,5-dimethyl-1,3,4-triazole was obtained by condensation of hydrazine with acetic acid.[34,35]

Paal–Knorr synthesis of *N*-benzyloxycarbonyl-*N*-amino pyrroles (1–4) and *N*-acetyl-*N*-amino pyrroles (5–8)

General procedure: a mixture of 5–15 g of the corresponding 1,4-diketone, either 1.1 mole equivalents of benzyloxycarbonylhydrazine (**1–4**) or 1.5 mole equivalents of acetylhydrazine (**5–8**), 40 mg of *p*-toluenesulfonic acid, and 120 ml toluene was heated in a Dean and Stark apparatus and refluxed overnight. During this period, the expected amount of H_2O (2 mole equivalents) separated from the reaction mixture. After removal of solvents on a rotary evaporator, a white crystalline residue was obtained. This was recrystallized from a mixture of chloroform/*n*-hexane (v/v = 1/5), yielding a white crystalline product in 37–89% yield. Spectroscopic data [^{1}H and ^{13}C NMR, IR, mass spectrometry (MS)] for **1–8** are in line with their structural features.

Table 2. Elemental analyses of metal complexes **31a–42b**

Compound	Formula	C: calc./found	H: calc./found	N: calc./found
31a	$C_{17}H_{17}Cl_2FeN_5$	48.8/48.0	4.1/3.8	16.8/16.0
31b	$C_{17}H_{17}Cl_2CoN_5$	48.5/47.7	4.1/3.6	16.6/15.8
32a	$C_{21}H_{25}Cl_2FeN_5$	53.2/52.7	5.3/5.4	14.8/13.9
32b	$C_{21}H_{25}Cl_2CoN_5$	52.8/52.3	5.3/5.1	14.7/14.3
32c	$C_{21}H_{25}Cl_3FeN_5$	49.5/48.6	4.9/4.8	13.7/12.5
33a	$C_{29}H_{41}Cl_2FeN_5$	59.4/58.3	7.0/6.4	11.9/10.4
33b	$C_{29}H_{41}Cl_2CoN_5$	59.1/58.8	7.0/6.8	11.9/10.4
33c	$C_{29}H_{41}Cl_3FeN_5$	56.0/55.3	6.7/6.3	11.3/10.3
34a	$C_{25}H_{33}Cl_2FeN_5$	56.6/56.0	6.3/6.0	13.2/12.0
34b	$C_{25}H_{33}Cl_2CoN_5$	56.3/56.5	6.2/6.6	13.1/11.5
35a	$C_{31}H_{29}Cl_2FeN_5$	62.2/61.4	4.9/5.1	11.7/11.5
35b	$C_{31}H_{29}Cl_2CoN_5$	61.9/60.2	4.9/4.7	11.6/11.0
36a	$C_{33}H_{33}Cl_2FeN_5$	63.3/63.2	5.3/5.5	11.2/11.0
36b	$C_{33}H_{33}Cl_2CoN_5$	63.0/62.3	5.3/5.0	11.1/10.5
37a	$C_{25}H_{21}Cl_2FeN_5$	57.9/57.2	4.1/3.9	13.5/12.9
37b	$C_{25}H_{21}Cl_2CoN_5$	57.6/56.8	4.1/3.7	13.4/12.5
38a	$C_{27}H_{25}Cl_2FeN_5$	59.4/58.6	4.6/4.6	12.8/11.5
38b	$C_{27}H_{25}Cl_2CoN_5$	59.0/58.5	4.6/4.4	12.8/11.7
39a	$C_{33}H_{25}Cl_2FeN_5$	64.1/62.9	4.1/4.1	11.3/10.0
39b	$C_{33}H_{25}Cl_2CoN_5$	63.8/62.8	4.1/4.5	11.3/9.7
40a	$C_{17}H_{21}Cl_2FeN_9$	42.7/22.3[a]	4.4/3.8[a]	26.4/10.4[a]
41a	$C_{27}H_{25}Cl_2FeN_5$	59.4/58.8	4.6/4.6	12.8/11.6
42b	$C_{18}H_{20}Cl_2CoN_4S$	47.6/46.8	4.4/3.7	12.3/11.1

[a] Experimental values correspond to a **40a** complex with approximately two additional equivalents of $FeCl_2$ coordinated to the 3,4-nitrogen atoms of the two triazole substituents.

Synthesis of *N*-amino pyrroles (9–16)

General deprotection protocol: a mixture of 5–15 g of the *N*-protected aminopyrrole (**1–8**) and an excess solid KOH was refluxed in 80 ml of ethylene glycol until no more starting material could be detected according to thin-layer chromatography (TLC) analysis. The reflux period varied from 1 to 36 h, depending on the steric bulk of the 2,5-substituents of the starting *N*-protected aminopyrrole. The mixture was cooled to room temperature, 200 ml of water was added, and the product was extracted into dichloromethane. Removal of solvent on a rotary evaporator yielded the crystalline product in 80–95% yield. Spectroscopic data (^{1}H and ^{13}C NMR, IR, MS) for **9–16** are consistent with their structural features.

Synthesis of bis-*N*-azolyl-2,6-bis(imino)pyridyl ligands (17–28)

General condensation procedure: a mixture of 2–6 g of *N*-aminoazole, 2,6-diacetylpyridine (2.2 mole equivalents of *N*-aminoazole/1 mole equivalent diacetylpyridine) was dissolved in a minimum amount of methanol and 1 ml formic acid was added. The mixture was stirred at room temperature and/or refluxed (2–48 h), depending on the reactivity of the aminoazole. In the case of aryl-substituted aminopyrroles it proved necessary to perform the condensation in refluxing propionic acid as solvent. After the reaction was shown by TLC analysis to be complete (in terms of bis-condensation or complete consumption of the corresponding monoimine), the product was separated by filtration, washed with small portions of methanol, and dried *in vacuo*, affording the product in approximately 90% yield. Spectroscopic data (^{1}H and ^{13}C NMR, IR, MS) for **17–28** are consistent with their structural features.

2,6-Diacetylpyridine-(carbazol-9-yl)-(2,5-dimethylpyrrol-1-yl)bisimine (29)

Synthesis of the monoimine

A mixture of 300 mg (2.7 mmol) diacetylpyridine, 375 mg (2.1 mmol) *N*-aminocarbazole, 15 ml methanol, and 0.1 ml formic acid was stirred at 0 °C for 1 h. The precipitated yellow monoimine was filtered off, washed with methanol, and chromatographed on silica, yielding 290 mg (0.89 mmol, 42%, m.p. 130–134 °C).

Synthesis of the 'mixed' bisimine

A mixture of 214 mg (0.65 mmol) carbazolylmonoimine, 71 mg (0.65 mmol) 2,5-dimethyl-*N*-aminopyrrole, 10 ml methanol, and 0.1 ml formic acid was stirred at 0 °C for 6 h.

The precipitated yellow bisimine was filtered off and washed with methanol. TLC analysis showed that only the 'mixed' bisimine was formed and none of the symmetric bisimines **18** or **25**. The product was dried *in vacuo*, affording 204 mg (0.50 mmol, 76.9%) of yellow powder with spectroscopic data (^{1}H and ^{13}C NMR, IR, MS) in accordance with its structure.

2,5-Diformylthiophene-bis(2,5-diisopropylpyrrol-1-yl)imine (30)

A mixture of 474 mg (2.9 mmol) 2,5-diisopropyl-*N*-aminopyrrole (**10**), 200 mg (1.4 mmol) 2,5-diformyl-thiophene, 10 ml methanol, and 0.5 ml formic acid was refluxed for 2 h. The precipitated yellow bisimine was filtered off, washed with methanol, and dried *in vacuo*, yielding 510 mg (1.2 mmol, 85.7%) of yellow powder with spectroscopic data (^{1}H and ^{13}C NMR, IR, MS) in accordance with its structure.

Synthesis of metal complexes (31a–42b) [a: M = Fe(II); b: M = Co(II); c: M = Fe(III)] of the ligands (17–30)

General procedure: a Schlenk tube was charged under an atmosphere of argon with 0.1–1.5 g of the appropriate ligand and 1 mole equivalent of the anhydrous metal chloride dissolved in dry 2-butanol (for $FeCl_2$), dichloromethane (for $FeCl_3$), or THF (for $CoCl_2$). The mixture was stirred at room temperature overnight or heated to 80 °C for a few hours. After removal of solvent the dark-colored product was washed with small portions of dry hexane and/or ether, filtered, and dried *in vacuo*, affording the paramagnetic complexes in 37–94% yield, which were characterized by elemental analysis (Table 2) and by mass and IR spectroscopy.

Table 3. Crystal data and structure refinement for **39a**

Molecular formula	$C_{33}H_{35}Cl_2FeN_5 \cdot 3CH_3CN \cdot 0.5C_6H_6$
Formula weight	628.42
Crystal system	triclinic
Space group	$P1$ (no. 2)
a (pm)	979.6(3)
b (pm)	1229.1(4)
c (pm)	1747.7(6)
α (deg)	81.44(2)
β (deg)	86.51(3)
γ (deg)	76.31(2)
V (nm^3)	2.0210(4)
Z	4
Temperature (K)	218(2)
d_{calcd} (Mg m^{-3})	1.283
Absorption coefficient (mm^{-1})	0.545
$F(000)$	810
Color, habit	black, plate
Crystal size (mm^3)	0.9 × 0.2 × 0.04
θ range for data collection (deg)	2.56–20.74
Index ranges	$0 \leq h \leq 9$ $-11 \leq k \leq 12$ $-17 \leq l \leq 17$
No. of reflections collected	4509
No. of independent reflections	4192 ($R_{int} = 0.0302$)
No. of reflections with $I > 2\,\sigma(I)$	2791
Refinement method	full-matrix least-squares on F^2
Data/restraints/parameters	3774/0/501
Goodness-of-fit on F^2	1.020
Final R indices $[I > 2\,\sigma(I)]$	$R_1 = 0.0507$, $wR_2 = 0.1013$
R indices (all data)	$R_1 = 0.0948$, $wR_2 = 0.1228$
Max diff peak/hole (e$^-$ nm^{-3})	279 and −199

Although the complexes in Table 2 were characterized by mass and IR spectroscopy, the elemental analysis results are not always close to the theoretical values. Regarding the catalytic performance of these (impure) metal complexes as precatalysts, there is a general point to be made: olefin polymerization of metal complexes has to be 'activated' by a 'cocatalyst' (MAO) that is actually present in large excess relative to the amount of precatalyst. Most important, not all of a given precatalyst is converted to the catalytically active site, and the function of MAO is at least fourfold: (i) to trap all protic species that might be present, either in the monomer or in the solvent, or as impurities in the precatalysts; (ii) to alkylate the metal halide precatalyst; (iii) to abstract a halide from the precatalyst to give a catalytically active cationic species; (iv) to delocalize the anionic charge in such a manner that a separated ion pair is obtained which can then perform its function as the actual catalyst. Therefore, the figures of merit of a given precatalyst are very dependent on experimental conditions, and the purity of the starting precatalysts is, in fact, not so critical as one might expect, because any impurities are trapped by the cocatalyst. Therefore, the performance of these systems under the usual industrial conditions (even starting from not ideally pure compounds) gives useful values, especially in direct comparison under identical experimental conditions with the Brookhart complex **A**.[8,9]

Olefin (ethylene/hexene/propylene) polymerizations

A three-necked round-bottomed flask with mechanical stirrer and gas inlet tube was charged with 150 ml (250 ml) of toluene. MAO solution (30% in toluene) was added to an amount to reach a ratio of 100:1 with respect to the metal complex added later. In copolymerizations, 12.5 ml (25 ml) 1-hexene was added at this time. Then 50 μmol (100 μmol) of the metal complex was added. At a temperature of 30 °C, the olefin flow of 40 l h^{-1} was adjusted. After 1 h the reaction was quenched by adding a mixture of 15 ml conc. HCl and 50 ml methanol. When a precipitate was formed, this precipitate was washed with methanol and dried *in vacuo*. When no precipitate was formed, the phases were separated and the polar phase was extracted with 100 ml of toluene. The organic layers were combined and the volatiles removed *in vacuo*. The details are summarized in Table 1.

SINGLE CRYSTAL X-RAY STRUCTURE DETERMINATION OF 39A

X-ray crystallographic data (Table 3) were collected using a Siemens P4 diffractometer with graphite-monochromatized MoKα radiation ($\lambda = 71.073$ pm). The unit cell parameters were determined from 25 randomly selected reflections, obtained by P4 automatic routines. Data were measured via ω-scan and corrected for Lorentz and polarization effects. The structure was solved by direct methods (SHELXS-86)[36] and refined by a full matrix least-squares procedure using F^2 (SHELXL-93).[37] The function minimized was $\sum[w(F_o^2 - F_c^2)^2]$ with the weight defined as $w^{-1} = [\sigma^2(F_o^2) + (xP)^2 + yP]$ and $P = (F_o^2 + 2F_c^2)/3$. All non-hydrogen atoms were refined with anisotropic displacement parameters. Hydrogen atoms were located by difference Fourier methods, but in the refinement they were included in calculated positions and refined with isotropic displacement parameters 1.2 times and 1.5 (for methyl hydrogen atoms) higher than U_{eq} of the attached atoms. Further details of the crystal structure investigation of **39a** have been deposited with the Cambridge Crystallographic Data Centre as supplementary publication no. CCDC-186444. Copies of the data can be obtained free of charge on application to CCDC, 12 Union Road, Cambridge CB2 1EZ, UK (fax: +44-1223-336033; telephone: +44-1223-336408; website: http://www.ccdc.cam.ac.uk).

Acknowledgements

We thank Stephan Lehmann, Polymer Laboratory of BASF, for NMR analysis; Heiko Maas, Ammonia Laboratory of BASF for GC-analysis; and Karl-Hans Ongania, Institute of Organic Chemistry, University of Innsbruck, for mass spectroscopic measurements.

REFERENCES

1. Britovsek GJP, Gibson VC and Wass DF. *Angew. Chem.* 1999; **111**: 448; *Angew. Chem. Int. Ed. Engl.* 1999; **38**: 428.
2. Ittel SD, Johnson LK and Brookhart M. *Chem. Rev.* 2000; **100**: 1169.
3. Mecking S. *Coord. Chem. Rev.* 2000; **203**: 325.
4. Mecking S. *Angew. Chem.* 2001; **113**: 550; *Angew. Chem. Int. Ed. Engl.* 2001; **40**: 534.
5. Britovsek GJP, Gibson VC, Kimberley BS, Maddox PJ, McTavish SJ, Solan GA, White AJP and Williams DJ. *Chem. Commun.* 1998; 849.
6. Britovsek GJP, Bruce M, Gibson VC, Kimberley BS, Maddox PJ, Mastroianni S, McTavish SJ, Redshaw C, Solan GA, Strömberg S, White AJP and Williams DJ. *J. Am. Chem. Soc.* 1999; **121**: 8728.
7. Britovsek GJP, Mastroianni S, Solan GA, Baugh SPD, Redshaw C, Gibson VC, White AJP, Williams DJ and Elsegood MRJ. *Chem. Eur. J.* 2000; **6**: 2221.
8. Small BL, Brookhart M and Bennett AMA. *J. Am. Chem. Soc.* 1998; **120**: 4049.
9. Small BL and Brookhart M. *Macromolecules* 1999; **32**: 2120.
10. Bennett AMA (DuPont). WO 98/27124, 1998.
11. Britovsek GJP, Dorer BA, Gibson VC, Kimberley BS and Solan GA (BA Chemicals Ltd). WO 99/12981, 1999.
12. Bennett AMA (DuPont). WO 99/51550, 1999.
13. Brookhart MS and Small BL (DuPont). WO 98/30612, 1998.
14. Deng L, Margl P and Ziegler T. *J. Am. Chem. Soc.* 1999; **121**: 6479.
15. Margl P, Deng L and Ziegler T. *Organometallics* 1999; **18**: 5701.
16. Griffiths EAH, Britovsek GJP, Gibson VC and Gould IR. *Chem. Commun.* 1999; 1333.
17. Schmid R and Ziegler T. *Organometallics* 2000; **19**: 2756.
18. Moody LS, Mackenzie PB, Killian CM, La Voie GG, Ponasik JA, Barrett AGM, Smith TW and Pearson JC (Eastman Chemical Company). WO 00/50470, 2000.
19. Britovsek GJP, Gibson VC, Kimberley BS, Mastroianni S, Redshaw C, Solan GA, White AJP and Williams DJ. *J. Chem. Soc., Dalton Trans.* 2001; 1639.
20. Gibson VC and McTavish SJ (BP Chemicals Ltd). WO 00/08034, 2000.
21. Bildstein B, Amort C, Malaun M, Kristen MO, Gonioukh A, Lilge D and Lehmann S (BASF AG). DE 19939415, 1999.
22. McLeod M, Boudreault N and Leblanc Y. *J. Org. Chem.* 1996; **61**: 1180.
23. Ito Y, Konoike T and Saegusa T. *J. Am. Chem. Soc.* 1975; **97**: 2912.
24. Fiandanese V, Marckese G, Martina V and Ronzini L. *Tetrahedron Lett.* 1984; **25**: 4805.
25. Cahiez G and Laboue B. *Tetrahedron Lett.* 1992; **33**: 4439.
26. Stetter H and Schreckenberger M. *Chem. Ber.* 1974; **107**: 2453.
27. Stetter H and Kuhlmann H. *Chem. Ber.* 1976; **109**: 3426.
28. Stetter H. *Angew. Chem.* 1976; **21**: 695.
29. Stetter H and Jonas F. *Chem. Ber.* 1981; **114**: 564.
30. Wallace RG. *Aldrichim. Acta* 1980; **13**(1): 3.
31. Somei M and Natsume M. *Tetrahedron Lett.* 1974; 461.
32. Davis L, Olsen G, Klein JT, Kapples K, Huger F, Smith C, Petko W, Cornfeldt M and Effland R. *J. Med. Chem.* 1996; **39**: 570.
33. Davis L, Olsen G, Klein JT, Kapples K, Huger F, Smith C, Petko W, Cornfeldt M and Effland R. *J. Med. Chem.* 1996; **39**: 582.
34. Herbst R and Garrison J. *J. Org. Chem.* 1953; **18**: 872.
35. Tarrago G, Marzin C, Najimi O and Pellegrin V. *J. Org. Chem.* 1990; **55**: 420.
36. Sheldrick GM. *SHELXS-86: Program for crystal structure solutions.* University of Göttingen, Göttingen, Germany, 1986.
37. Sheldrick GM. *SHELXS-93: Program for the refinement of crystal structures.* University of Göttingen, Göttingen, Germany, 1993.